Effect of undulations on spontaneous braid formation

Dominic Lee*
Department of Chemistry, Imperial College London, London SW7 2AZ, United Kingdom
(Received 1 March 2013; published 29 August 2013)

This paper is an extension of a recent study where it was shown that forces dependent on molecular helical structure may cause two DNA molecules to spontaneously braid [R. Cortini *et al*., Biophys. J. **101**, 875 (2011)]. Here, bending fluctuations of molecular center lines about the braid axis are incorporated into the braiding theory, which may be generalized to other helix-dependent interactions and other helical molecules. The free energy of the pair of molecules is recalculated and compared to its value without incorporating undulations. We find that the loss of configurational entropy due to confinement of the molecules in the braid is quite high. This contribution to the free energy increases the amount of attraction needed for spontaneous braiding due to helix-dependent forces. The theory will be further developed for plectonemes and braids under mechanical forces in later work.

DOI: 10.1103/PhysRevE.88.022719 PACS number(s): 87.15.K−, 05.20.−y, 82.35.Pq, 36.20.Ey

I. INTRODUCTION

In a recent paper [1] the possibility of two DNA molecules spontaneously braiding through interactions, specific to the helical structure of the molecules, was investigated. It was found that, as DNA is a right handed molecule, helix-specific interactions favor a left handed braid. This was also argued from simulation and x-ray scattering data in the work of Timsit and Varnai [2]. One of the limitations of Ref. [1] is that it was a ground-state calculation in terms of the bending degrees of freedom, and thus could not estimate the confinement entropy reduction due to loss of such fluctuation modes. This current work attempts to address this issue by incorporating undulations, thereby developing a more complete theory for molecular braids with helix-specific interactions.

In the past, statistical mechanical theories have been developed to deal with undulations in braids and plectonemes of semiflexible rodlike molecules [3,4]. These theories rely on the assumption that we can treat the molecules as uniformly charged rods. On the other hand, interaction theories have been proposed [5–8] that incorporate helical charge distributions to describe forces between parallel, cylindrical molecules. The most important qualitative feature of these theories is their dependence on how the helical charge distributions are azimuthally orientated about the long axes of the molecules. The Kornyshev-Leikin (KL) theory [5,6] assumes mean-field electrostatics with a bulk dielectric response, where interactions between the individual small ions are neglected. Conversely, in the work of Ref. [7], the effect of helical charge distributions was investigated in the limit of strong correlations between the small ions in solution about two helically charged molecules. Finally, Ref. [8] considered corrections to the KL theory due to ion correlations and steric effects. In these works a significant dependence of the interaction potential on the azimuthal orientation of the molecules was seen, at close enough distances and at certain values of the various model parameters. All of these helix-dependent theories give rise to the possibility of spontaneous braid formation, arising from the appearance of a chiral torque that causes the molecules to wrap around each other due to their helical nature [1,2]. Perhaps more importantly, this chiral torque may also give rise to a preferred handedness for both plectonemes [9] and for mechanically generated braids, under certain conditions. One method for mechanically braiding molecules is discussed in Ref. [10], where a very slight asymmetry between left and right handed braids has indeed been observed in monovalent salt solution.

Could there be cases where helix-dependent forces significantly influence equilibrium properties of a molecular braid or plectoneme? For assemblies and toroidal structures formed by DNA, in the presence of condensing agents, there is evidence to suggest that helical structure does indeed matter. The decay lengths of the forces between molecules from experiments [11–13] agree well with the KL theory [5,6,14], where these lengths arise from the helical structure, and the osmotic pressure is fitted reasonably well by the results of Ref. [14] as a function of distance. In addition, there is evidence of azimuthal order [15–17], a preferred orientation for each DNA molecule or segment about its long axis [14]. Therefore, it does not seem unreasonable to expect, in certain cases, that helical structure might matter in the formation of DNA braids and plectonemes, and perhaps those formed by other charged, helical molecules. However, this still remains to be seen experimentally.

For a complete description of braids with helix-dependent forces, a fully consistent theory, the statistical mechanics describing undulation effects [3,4] needs to be modified. This needs to take account of nontrivial effects to do with the molecular twisting degrees of freedom, as well as the chiral (braiding) torque [1,2] that arises from forces that depend on the helical structure of the molecule. In assemblies of DNA, a full statistical mechanical theory of undulations and twisting was developed [14], taking into account both helix-dependent forces and steric confinement. This theory built on the works of [18–21] that dealt with undulations and confinement of the molecules. With some modifications these developments could be applied to braids.

Making such modifications, we consider here the simplest case of braids only stabilized by helix-dependent forces. The main purpose of this work is to provide an important stepping stone for a consistent statistical mechanical treatment of braids, formed of helical molecules, under additional factors of topology and mechanical forces. This is particularly interesting as such braids are indeed known to form in nature. An

*domolee@hotmail.com

important example is a DNA plectoneme structure formed by plasmids in bacteria. Also, in improving the theory of Ref. [1], we examine what effect undulations have on spontaneous braid formation. Therefore, the helix-dependent interaction model we choose for numerical calculations is the KL theory. Nevertheless, the whole approach can be modified to any interaction theory where the helical structure of the molecules forming the braid is important. It could be easily adapted to the strong correlation theory of Ref. [7] or an empirical theory constructed from simulation results, such as those of Ref. [2].

The main paper is divided into three further sections. In the theory section we discuss how the braid geometry can be described mathematically, using an approach similar to Ref. [22]. Next, using results of the Supplemental Material and electrostatic calculations [1,23], we write down a partition function that describes the thermal fluctuations of the braid and how steric effects can be estimated using a similar approach to Ref. [14]. Finally, we outline a variational approximation using the Gibbs- Bogoliubov inequality and present an expression for the free energy in terms of the variational parameters, each of which has clear physical meaning. In the Results section, we calculate the free energy, parameters that define the average braid structure, and quantities that characterize the size of fluctuations about the mean braid structure. We do this calculation for braids formed of DNA molecules with the same base-pair text (homologous sequences) and those with two completely random sequences. We compare these results against the case where braid undulations are not included. Lastly, in the Discussion section we discuss the significance of the results, the limitations of the theory, and point to new work.

II. THEORY

A. Specifying fluctuating braid geometry

We will consider a fluctuating braid where the braid axis is still assumed to be straight; undulations of this axis will be considered in a later work. This assumption is on a par with the theories of [3,4]. The braid axis can be written as $\mathbf{r}_A(z) = z(s)\hat{\mathbf{k}}$ (in a reference frame spanned by the usual Cartesian unit vectors $\{\hat{\mathbf{i}},\hat{\mathbf{j}},\hat{\mathbf{k}}\}$), and the molecular center lines of the molecules (labeled 1 and 2) can be written as

$$\begin{aligned}\mathbf{r}_1(s) &= z(s)\hat{\mathbf{k}} - \frac{R(s)\hat{\mathbf{d}}(s)}{2},\\ \mathbf{r}_2(s) &= z(s)\hat{\mathbf{k}} + \frac{R(s)\hat{\mathbf{d}}(s)}{2}.\end{aligned} \tag{2.1}$$

$\hat{\mathbf{d}}(s)$ is a vector that points along a line of length $R(s)$ that connects the two molecular center lines. This line is perpendicular to, as well as bisected by, the braid axis so that $\hat{\mathbf{d}}(s)\cdot\hat{\mathbf{k}} = 0$ (see Fig. 1). Here, s is a unit arc-length coordinate that runs from $-L/2$ to $L/2$, where L is the contour length of the molecule. The tangent vectors are defined through $\hat{\mathbf{t}}_1(s) = \mathbf{r}'_1(s)$ and $\hat{\mathbf{t}}_2(s) = \mathbf{r}'_2(s)$ (where the prime, here, stands for differentiation with respect to argument). One should note that $z(s)$, $R(s)$, and $\hat{\mathbf{d}}(s)$ are not independent of each other, as we have the unitary requirement $|\hat{\mathbf{t}}_1(s)| = |\hat{\mathbf{t}}_2(s)| = 1$. By

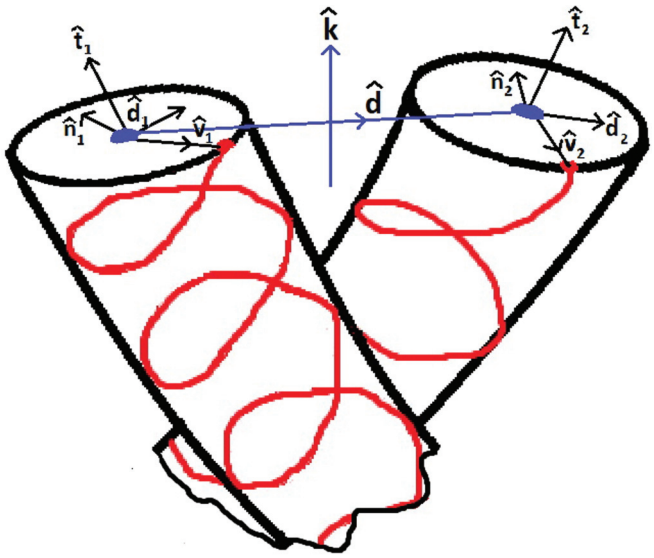

FIG. 1. (Color online) Diagram showing part of the braid formed by two molecules. Here, the red (gray) lines trace out the position of the minor groove in a distorted helical pattern. This distortion is due to thermal fluctuations and base-pair clashes. The blue (gray) dots represent the DNA center lines. A blue (gray) line of length $R(s)$, perpendicular to the braid axis that points along the z axis, connects the two center lines. The unit vector $\hat{\mathbf{d}}(s)$ lies on this line connecting the molecules. Two braid frames can describe the orientation of the DNA cross sections (at fixed values of s) relative to the line connecting the two center lines, described by the basis sets $\{\hat{\mathbf{d}}_1,\hat{\mathbf{n}}_1,\hat{\mathbf{t}}_1\}$ and $\{\hat{\mathbf{d}}_2,\hat{\mathbf{n}}_2,\hat{\mathbf{t}}_2\}$. The orientation of the minor grooves can be described, with respect to these frames, by Eq. (2.7).

constructing other unit vectors

$$\hat{\mathbf{n}}_1(s) = \frac{\hat{\mathbf{t}}_1(s)\times\hat{\mathbf{d}}(s)}{|\hat{\mathbf{t}}_1(s)\times\hat{\mathbf{d}}(s)|}, \quad \hat{\mathbf{d}}_1(s) = \hat{\mathbf{n}}_1(s)\times\hat{\mathbf{t}}_1(s), \tag{2.2}$$

$$\hat{\mathbf{n}}_2(s) = \frac{\hat{\mathbf{t}}_2(s)\times\hat{\mathbf{d}}(s)}{|\hat{\mathbf{t}}_2(s)\times\hat{\mathbf{d}}(s)|}, \quad \hat{\mathbf{d}}_2(s) = \hat{\mathbf{n}}_2(s)\times\hat{\mathbf{t}}_2(s), \tag{2.3}$$

we may construct two local orthogonal frames called the *braid frames* [22] spanned by the basis sets $\{\hat{\mathbf{d}}_1,\hat{\mathbf{n}}_1,\hat{\mathbf{t}}_1\}$ and $\{\hat{\mathbf{d}}_2,\hat{\mathbf{n}}_2,\hat{\mathbf{t}}_2\}$. One should note only when $R'(s) = 0$ is $\hat{\mathbf{d}}_1(s) = \hat{\mathbf{d}}_2(s) = \hat{\mathbf{d}}(s)$, otherwise all three vectors point in different directions (see Fig. 1). We define the tilt angle $\eta(s)$ through the following relation between tangent vectors:

$$\hat{\mathbf{t}}_1(s)\cdot\hat{\mathbf{t}}_2(s) = \cos\eta(s). \tag{2.4}$$

As $\hat{\mathbf{d}}(s)$ is perpendicular to $\hat{\mathbf{k}}$, we may parametrize it as

$$\hat{\mathbf{d}}(s) = \cos\theta(s)\hat{\mathbf{i}} + \sin\theta(s)\hat{\mathbf{j}}, \tag{2.5}$$

where $\theta(s)$ is the angle $\hat{\mathbf{d}}(s)$ makes with the x axis in the reference frame. If $R'(s) \ll 1$ one may show (see Appendix A of Ref. [24]) that the rate of precession of $\hat{\mathbf{d}}(s)$ can be related to the braid tilt angle $\eta(s)$ through the expression

$$\frac{R(s)}{2}\frac{d\theta(s)}{ds} \simeq -\sin\left(\frac{\eta(s)}{2}\right). \tag{2.6}$$

In the braid frames, we can describe the relative orientation of the helices (for DNA, the position of the minor groove)

through the vectors (see Fig. 1)

$$\hat{\mathbf{v}}_1(s) = \cos\phi_1(s)\hat{\mathbf{d}}_1(s) + \sin\phi_1(s)\hat{\mathbf{n}}_1(s),$$
$$\hat{\mathbf{v}}_2(s) = \cos\phi_2(s)\hat{\mathbf{d}}_2(s) + \sin\phi_2(s)\hat{\mathbf{n}}_2(s). \tag{2.7}$$

Then, the positions of the helices forming the braid may be described by the vectors

$$\mathbf{r}_{H1}(s) = \mathbf{r}_1(s) + a\hat{\mathbf{v}}_1(s) \quad \text{and} \quad \mathbf{r}_{H2}(s) = \mathbf{r}_2(s) + a\hat{\mathbf{v}}_2(s), \tag{2.8}$$

where a is the helix radius. It is also useful to define the twist densities

$$g_1(s) = \hat{\mathbf{u}}_1(s) \cdot \frac{d\hat{\mathbf{v}}_1(s)}{ds} \quad \text{and} \quad g_2(s) = \hat{\mathbf{u}}_2(s) \cdot \frac{d\hat{\mathbf{v}}_2(s)}{ds}, \tag{2.9}$$

where $\hat{\mathbf{u}}_1(s) = \hat{\mathbf{t}}_1(s) \times \hat{\mathbf{v}}_1(s)$ and $\hat{\mathbf{u}}_2(s) = \hat{\mathbf{t}}_2(s) \times \hat{\mathbf{v}}_2(s)$. The twist densities $g_1(s)$ and $g_2(s)$ are geometric quantities that measure the rates of precession of the vectors $\hat{\mathbf{v}}_1(s)$ and $\hat{\mathbf{v}}_2(s)$ about their tangent vectors $\hat{\mathbf{t}}_1(s)$ and $\hat{\mathbf{t}}_2(s)$, respectively. These geometric quantities are important when we consider the elastic terms that limit the deformation of the two helices, due to thermal fluctuations and helix-specific interactions between the molecules. Most importantly, for ideal helices, the rates of precession of the helices around the tangent vector of molecular center line are constant, i.e., $g_1(s) = g_1^0$ and $g_2(s) = g_2^0$, where both g_1^0 and g_2^0 do not depend on s. When $R'(s) \ll 1$ we find that

$$g_1(s) \approx \frac{d\phi_1(s)}{ds} - \frac{\sin\eta(s)}{R} \quad \text{and}$$
$$g_2(s) \approx \frac{d\phi_2(s)}{ds} - \frac{\sin\eta(s)}{R}. \tag{2.10}$$

B. Elastic energy

The energy of the system can be written as the sum of the elastic energies of the two molecules, the interaction energy, and a steric term

$$E_T = E_{\text{elst}} + E_{\text{int}} + E_{\text{st}}. \tag{2.11}$$

In this section we consider the elastic energy. The sum of the two elastic energies of the molecules of length L is given by (for more details see Ref. [14])

$$\frac{E_{\text{elst}}}{k_BT} = \int_{-L/2}^{L/2} ds \left(\frac{l_p^b}{2} \left[\left(\frac{d\hat{\mathbf{t}}_1(s)}{ds} \right)^2 + \left(\frac{d\hat{\mathbf{t}}_2(s)}{ds} \right)^2 \right] + \frac{l_p^h}{2} \left\{ \left[g_1(s) - g_1^0(s) \right]^2 + \left[g_2(s) - g_2^0(s) \right]^2 \right\} \right). \tag{2.12}$$

The bending persistence length $l_p^b = B/k_BT$ is a measure of the rigidity of the molecules to bending through deformations of their center lines. For DNA we use the value $l_p^b \approx 500$ Å. The helical persistence length l_p^h is a measure of the rigidities of the helices with respect to distortions due to twisting and stretching. It is given by $l_p^h = C_tC_s/(C_s + \bar{g}^2C_t)k_BT$ [14], where C_t, C_s, and $\bar{g}$ are the twisting rigidity, stretching rigidity, and average value of both $g_1^0(s)$ and $g_2^0(s)$, respectively. We estimate $l_p^h \approx 400$ Å, for DNA, based on a torsional rigidity of $C_t/k_BT \approx 1000$ Å measured in recent twisting experiments [25] and a value of $C_s \approx 10^{-4}$ dyn [6].

In Eq. (2.12) we have not included contributions due to stretching fluctuations along the helical lines $\mathbf{r}_{H1}(s)$ and $\mathbf{r}_{H2}(s)$. These fluctuation modes are unimportant, provided that the dominant contribution to the interaction energy comes from assuming the helices to be continuous, as opposed to a line of discrete points along the helices. This discreteness contributes additional modes to the interaction energy [6]. For DNA, as the negative charge is distributed on individual phosphate groups, indeed, such discrete modes should exist. However, these modes decay rapidly with R and are likely to be strongly suppressed by thermal fluctuations (as discussed in Ref. [6]), so we neglect them. One may also consider rigid body fluctuations such as sliding and rotation of the molecules. For such fluctuations, if they are limited by helix-dependent interactions, their size is roughly inversely proportional to the length of the molecules, L [6] (not accounting for molecular defects). Therefore, if the molecules are sufficiently long, the contribution from these modes of fluctuations is small, and in this study we do not include them.

We have now chosen the twist densities in the unstressed states to be $g_1^0(s)$ and $g_2^0(s)$, s-dependent quantities, which reflect some intrinsic disorder in the unstressed state of the helices. In other words, we allow for the ground-state ($T = 0$) configuration of the molecules to be irregular helices. For a braid composed of DNA, or some other helical heteropolymer, the local twist densities of the unstressed states are given by [14]

$$g_1^0(s) = \Delta g_1(s) + \bar{g} = \frac{\Omega_1^0(s) - \bar{g}h_1^0(s)}{\langle h \rangle} + \bar{g},$$
$$g_2^0(s) = \Delta g_2(s) + \bar{g} = \frac{\Omega_2^0(s) - \bar{g}h_2^0(s)}{\langle h \rangle} + \bar{g}, \tag{2.13}$$

where $\langle h \rangle$ is the average rise between base pairs. Here, both $\Omega_1^0(s)$ and $\Omega_2^0(s)$ are continuum representations of the patterns of twist angles (the relative angle of rotation about the molecular center line that one base pair makes with a neighboring base pair [26]) for molecules 1 and 2 in their relaxed states, respectively. The functions $h_1^0(s)$ and $h_2^0(s)$ are continuum representations of the patterns of rises (the distance along the molecular center line between neighboring base pairs [26]) for molecules 1 and 2. For DNA, these patterns of rise and twist angle depend on the sequence of base pairs and are disordered. This is due to steric clashes between neighboring base pairs [27]. The sequence dependence arises because each of the four base pairs has a different optimal shape. The average value of the twist density $\bar{g}$ is related to the average helical pitch H through $\bar{g} = 2\pi/H$. For DNA, we choose the value $H \approx 33.8$ Å. Over sufficiently large length scales, the intrinsic structural fluctuations $\Delta g_1(s)$ and $\Delta g_2(s)$ can be considered to have a Gaussian distribution over all realizations (base-pair texts) and uncorrelated in s [28]. This means that

$$\langle \Delta g_1(s)\Delta g_1(s') \rangle_{g_1} = \langle \Delta g_2(s)\Delta g_2(s') \rangle_{g_2} = \frac{1}{\lambda_c^{(0)}} \delta(s - s'), \tag{2.14}$$

$$\langle \Delta g_1(s) \rangle_{g_1} = \langle \Delta g_2(s) \rangle_{g_2} = 0. \tag{2.15}$$

Here, we define the intrinsic helical coherence length $\lambda_c^{(0)}$ as a measure of the disorder due to the intrinsic (nonthermal) distortions away from an ideal helix. Indeed, $1/\lambda_c^{(0)}$ is the width of the Gaussian distributions of both $\Delta g_1(s)$ and $\Delta g_2(s)$; also, for an ideal molecular helix in its ground state, $\lambda_c^{(0)} = \infty$. Here, the subscripts g_1 and g_2 on the averaging brackets denote that these are ensemble averages over all possible base-pair realizations of $g_1(s)$ and $g_2(s)$, not a thermal average. We can then distinguish between two particular cases of helical molecules forming a braid. One case, homologous molecules, is where both molecules have roughly the same intrinsic pattern of twist and rise, i.e., $g_1^0(s) = g_2^0(s)$. The second case, nonhomologous molecules, is where the molecules have a different pattern, i.e., $g_1^0(s) \neq g_2^0(s)$. If we take two nonhomologous molecules in their ground state, where there are no helix-dependent interactions between them, $\lambda_c^{(0)}$ is the length scale at which the two helices, with different base-pair texts, start to fall out of register with each other [29] when thermal fluctuations are not included.

It is useful for us to define $\Delta\Phi(s) = \phi_1(s) - \phi_2(s)$ and $\bar{\phi}(s) = \phi_1(s) + \phi_2(s)$. For relatively small tilt angles, $\bar{\phi}(s)$ is unimportant and can be effectively decoupled from the problem provided that the helical persistence length l_p^h is sufficiently large (see Appendix A of Ref. [24]). The elastic energy can then be approximated as the following (Appendix A of Ref. [24]), provided that $R'(s) \ll \cos\eta(s)$:

$$E_{\rm elst}[R(s),\eta(s),\Delta\Phi(s)] \approx k_B T \int_{-L/2}^{L/2} ds\, \mathsf{E}_{\rm elst}[\Delta\Phi'(s),R''(s),R'(s),R(s),\eta'(s),\eta(s)], \tag{2.16}$$

where

$$\begin{aligned}\mathsf{E}_{\rm elst}[\Delta\Phi'(s),R''(s),R'(s),R(s),\eta'(s),\eta(s)] = \Bigg[&\frac{l_p^h}{4}\left(\frac{d\Delta\Phi(s)}{ds} - \frac{\sigma_H\Delta\Omega(s)}{\langle h\rangle}\right)^2 + \frac{l_p^b}{4}\left(\frac{d^2R(s)}{ds^2}\right)^2 + \frac{l_p^b}{4}\left(\frac{d\eta(s)}{ds}\right)^2 \\ &+ \frac{l_p^b[1-\cos\eta(s)]^2}{R(s)^2} - \frac{l_p^b[1-\cos\eta(s)]}{2R(s)^2}\left(\frac{dR(s)}{ds}\right)^2 \\ &+ \frac{3l_p^b\sin\eta(s)}{2R(s)}\left(\frac{dR(s)}{ds}\right)\left(\frac{d\eta(s)}{ds}\right)\Bigg].\end{aligned} \tag{2.17}$$

Here, σ_H is a factor that is either $\sigma_H = 0$, for homologous molecules, or $\sigma_H = 1$, for nonhomologous molecules. When the molecules are nonhomologous, the function $\Delta\Omega(s) = \langle h\rangle[g_1^0(s) - g_2^0(s)]$ becomes important. This is a random Gaussian field that represents the base-pair mismatch between two nonhomologous DNA molecules. From Eqs. (2.14) and (2.15) we find that

$$\langle\Delta\Omega(s)\Delta\Omega(s')\rangle_{\Delta\Omega} = \frac{2\langle h\rangle^2}{\lambda_c^{(0)}}\delta(s-s'), \quad \langle\Delta\Omega(s)\rangle_{\Delta\Omega} = 0. \tag{2.18}$$

Here, the averaging bracket $\langle\cdots\rangle_{\Delta\Omega}$ corresponds to an ensemble average over all the realizations of $\Delta\Omega(s)$.

C. Interaction energy

We may parametrize the position vector describing surfaces of the molecule in the following way:

$$\begin{aligned}\mathbf{r}_{S1}(s,\varphi) &= \mathbf{r}_1(s) + a\hat{\mathbf{N}}_1(s,\varphi) \quad \text{and} \\ \mathbf{r}_{S2}(s,\varphi) &= \mathbf{r}_2(s) + a\hat{\mathbf{N}}_2(s,\varphi),\end{aligned} \tag{2.19}$$

where the surface normal vectors are given by

$$\begin{aligned}\hat{\mathbf{N}}_1(s,\varphi) &= \cos[\phi_1(s)+\varphi]\hat{\mathbf{d}}_1(s) + \sin[\phi_1(s)+\varphi]\hat{\mathbf{n}}_1(s), \\ \hat{\mathbf{N}}_2(s,\varphi) &= \cos[\phi_2(s)+\varphi]\hat{\mathbf{d}}_2(s) + \sin[\phi_2(s)+\varphi]\hat{\mathbf{n}}_2(s),\end{aligned} \tag{2.20}$$

and $0 \leqslant \varphi < 2\pi$. Here φ is an azimuthal coordinate, tracing out the circumference of the molecule, measured relative to either $\hat{\mathbf{v}}_1(s)$ or $\hat{\mathbf{v}}_2(s)$ [see Eq. (2.7)], depending on what molecule is considered. As a starting point for model calculations, the interaction energy between the two molecules may be written as

$$E_{\rm int} = \mathsf{E}[R(s)] - \mathsf{E}[\infty], \tag{2.21}$$

$$\begin{aligned}\mathsf{E}[R(s)] = &\int_{-L/2}^{L/2} ds \int_{-L/2}^{L/2} ds' \int_0^{2\pi} d\varphi \int_0^{2\pi} d\varphi' \sigma_1(\varphi) \\ &\times G[\mathbf{r}_{S1}(s,\varphi),\mathbf{r}_{S2}(s',\varphi')]\sigma_2(\varphi') \\ &+ \frac{1}{2}\sum_{\mu=1}^{2}\int_{-L/2}^{L/2} ds \int_{-L/2}^{L/2} ds' \int_0^{2\pi} d\varphi \\ &\times \int_0^{2\pi} d\varphi' \sigma_\mu(\varphi) G[\mathbf{r}_{S\mu}(s,\varphi),\mathbf{r}_{S\mu}(s',\varphi')]\sigma_\mu(\varphi').\end{aligned} \tag{2.22}$$

The functions $\sigma_1(\varphi)$ and $\sigma_2(\varphi')$ are the surface charge densities (or surface densities of another quantity, which has helical symmetry that determines the interaction between molecules). Here, $G(\mathbf{r},\mathbf{r}')$ (the Green's function) is a potential generated from a point positioned at $\mathbf{r}'$. In Eq. (2.22) this point is assumed to lie on one of the surfaces. The function $G(\mathbf{r},\mathbf{r}')$ may contain a highly nontrivial implicit functional dependence on the water-molecule interface that can be described by the surfaces given by Eq. (2.19). For the mean-field KL theory [5], $G(\mathbf{r},\mathbf{r}')$ is an electrostatic potential of a point charge at $\mathbf{r}'$ and $E[R(s)]$ is the electrostatic energy of the braid. Here, a nonlinear screening [or Manning condensed layer] is

incorporated in both $\sigma_1(\varphi)$ and $\sigma_2(\varphi')$, as well as a contribution from chemiadsorbed ions lying in the grooves. Then, $G(\mathbf{r},\mathbf{r}')$ is assumed to satisfy the linear Poisson-Boltzmann equation

$$-\nabla^2 G(\mathbf{r},\mathbf{r}') + \kappa_D^2 G(\mathbf{r},\mathbf{r}') = \frac{4\pi\delta(\mathbf{r}-\mathbf{r}')}{\varepsilon_w}, \tag{2.23}$$

where ε_w is the bulk dielectric constant of the surrounding solvent and κ_D is the inverse Debye screening length. The dielectric constant of molecular cores [in the regions enclosed by $\mathbf{r}_{S1}(s,\varphi)$ and $\mathbf{r}_{S2}(s,\varphi)$], ε_c is considered to be such that $\varepsilon_c \ll \varepsilon_w$ At the surfaces $\mathbf{r}_{S1}(s,\varphi)$ and $\mathbf{r}_{S2}(s,\varphi)$, described by Eq. (2.19), the usual electrostatic boundary conditions apply; i.e., the continuity of electrostatic potential and the continuity of the component of the electrostatic displacement field (or induction) $\mathbf{D}(\mathbf{r})$ normal to the surface of the interface, as can be found in any textbook on electrostatics [30].

In Ref. [1], the electrostatic energy for a uniform braid where $R(s) = R_0$, $\eta(s) = \eta_0$, where R_0 and η_0 are constant values, was calculated using Eqs. (2.19)–(2.23) for small values of $\sin\eta_0$. It was justified (as well as extended to more general cases) in Ref. [23] that we can simply make R, $\Delta\Phi$, and η all s dependent within the expressions calculated in Ref. [1], provided that the braid axis is straight and $R'(s) \ll 1$ (this criterion we will justify later). This yields the following form for the interaction energy:

$$E_{\rm int}[R(s),\eta(s),\Delta\Phi(s)] = k_B T \int_{-L/2}^{L/2} ds \mathsf{E}_{\rm int}[\Delta\Phi(s),R(s),\eta(s)], \tag{2.24}$$

$$\mathsf{E}_{\rm int}[\Delta\Phi(s),R(s),\eta(s)] = \left(E_{\rm img}[R(s)] + \sum_{n=0}^{2} \left\{ E_0^{(n)}[R(s)] + \sin\eta(s) E_1^{(n)}[R(s)] \right\} \cos n\Delta\Phi(s) \right). \tag{2.25}$$

For the KL theory for the braid [1] the interaction coefficients are

$$E_{\rm img}(R) = -\frac{2l_B}{l_c^2} \sum_{n=-\infty}^{\infty} \sum_{j=-\infty}^{\infty} \frac{K_{n-j}(\kappa_n R) K_{n-j}(\kappa_n R)}{[\kappa_n a K_n'(\kappa_n a)]^2} \times \frac{I_j'(\kappa_n a)}{K_j'(\kappa_n a)} \zeta_n^2, \tag{2.26}$$

$$E_0^{(0)}(R) = \frac{2l_B(1-\theta)^2}{l_c^2} \frac{K_0(\kappa_D R)}{[\kappa_D a K_1(\kappa_D a)]^2}, \tag{2.27}$$

$$E_0^{(n)}(R) = \frac{4l_B}{l_c^2} \frac{(-1)^n K_0(\kappa_n R)}{[\kappa_n a K_n'(\kappa_n a)]^2} \zeta_n^2 \quad \text{for } n \neq 0, \tag{2.28}$$

$$E_1^{(n)}(R) = \frac{4l_B n^2 a \bar{g}}{l_c^2} \frac{(-1)^n K_1(\kappa_n R)}{[K_n'(\kappa_n a)]^2 (\kappa_n a)^3} \zeta_n^2, \tag{2.29}$$

where $\kappa_n = \sqrt{\kappa_D^2 + n^2 \bar{g}^2}$, $\bar{g} = 2\pi/H$, and the form factors ζ_n are the helical Fourier components (modes) of the molecular surface charge densities $\sigma_1(\varphi)$ and $\sigma_2(\varphi)$ [6], which are assumed to be the same for the two molecules [i.e., $\sigma_1(\varphi) = \sigma_2(\varphi)$]. For DNA, a simple model of counterion binding and condensation gives the form factor

$$\zeta_n(f_1,f_2,\theta) = \delta_{n,0}\theta(1-f_1-f_2) + \theta[f_1 + (-1)^n f_2] - \cos n\tilde{\phi}_s \tag{2.30}$$

(for other possible form factors see [6]). Here, l_c is the mean separation per unit charge (for DNA $l_c = \langle h \rangle/2 \approx 1.7$ Å), l_B is the Bjerrum length (taken to be 7 Å at room temperature). The parameters κ_D, a, and $\tilde{\phi}_s$ are the inverse Debye screening length, the effective cylinder, radius and the half-width of the minor groove, respectively. For DNA, we choose the values of $a \approx 11.2$ Å and $\tilde{\phi}_s \approx 0.4\pi$. The functions $I_n(x)$ and $K_n(x)$ are modified Bessel functions of the first and second kinds of order n. The functions $I_n'(x)$ and $K_n'(x)$ are their respective derivatives with respect to argument. The parameter θ is the fraction of the molecule neutralized by counterions and, for DNA, f_1 and f_2 are the relative proportions of ions localized in the minor and major grooves, respectively.

The size of the parameters θ, f_1, and f_2 depend on the particular species of ion(s). One factor that contributes to θ is the nonlinear screening layer from the Manning condensation of ions. As the valance of counterions in the solution about the DNA is increased, θ increases. For isolated DNA molecules in the limit of infinite dilution ($\kappa_D \to 0$), we have $\theta \approx 0.7$ for monovalent ions and $\theta \approx 0.9$ for trivalent ions [6,26]. Ions can also be electrostatically localized near the grooves, thereby causing f_1 and f_2 to be nonzero. In addition, there can be base-pair-specific chemi-adsorption inside the grooves. Transition metal ions such as manganese bind in a highly sequence-dependent way inside the DNA grooves [31]; there is even evidence to suggest that sodium ions feel a weak attractive potential in the minor groove of DNA for AT sequences [6]. Another complicating issue in the determination of these parameters is the highly nontrivial dielectric response of water near the DNA surface, where clearly a bulk dielectric response is inappropriate. We are also faced with an additional difficulty, which is that θ, f_1, and f_2 are intrinsic to the smooth cylinders considered in the model; in principle, counterion charge distributions for real DNA should be able to be mapped onto this model, but this along with the other issues makes the determination of the precise values of f_1, f_2, and θ very difficult. Therefore, we treat these model parameters as phenomenological. However, we might expect, for a monovalent salt solution $\theta \sim 0.4$–0.7 and perhaps for divalent ions $\theta \sim 0.6$–0.8, depending on the salt concentration and binding energies of the ions to the grooves.

We should emphasize that the overall form of Eq. (2.25) is not restricted to KL theory [Eqs. (2.26)–(2.30)] alone. In the spirit of the Ginzburg-Landau theory, its form can be argued heuristically from geometric and symmetry considerations for helix-specific interactions [not necessarily relying on calculations from Eq. (2.22)], provided that $R(s)$, $\sin\eta(s)$, and $\Delta\Phi(s)$ vary slowly compared with the inverse decay ranges of the interaction. Indeed, the coefficients $E_0^{(n)}(R)$ and $E_1^{(n)}(R)$ may be fitted to simulations or determined from an alternative theory where helical symmetry is important.

D. The steric interaction

The simplest way to model the steric term is to assume that molecules are smooth, hard cylinders so that

$$E_{\rm st}[R(s)] = 0 \quad \text{when} \quad R(s) > 2a, \tag{2.31}$$

$$E_{\rm st}[R(s)] = \infty \quad \text{when} \quad R(s) \leqslant 2a. \tag{2.32}$$

This may be quite a reasonable approximation, provided that the helix-specific interactions are strong, as considered here. In addition, we find, for the range of parameters that we investigate using the KL theory, the electrostatic interaction confines the molecules very strongly, i.e., it strongly suppresses undulations of the molecules within the braid. This makes effective steric interaction from smooth cylinders, arising from undulations, also a small contribution, as the molecules have little chance of colliding with each other. All of this would suggest that any contribution due to the helical shape of the molecules is likely to be a second order effect, for the electrostatic interaction model used and the range of parameters explored. Here, the main role of steric repulsion is to provide a cutoff that prevents overestimation of the enhancement of the interactions from undulations, which a smooth cylinder model should be sufficient in providing.

E. Approximating steric effects

In principle, using the energy functional given by Eqs. (2.11), (2.16), (2.17), (2.24), (2.25), (2.31), and (2.32), we could construct the partition function. However, in practice, to make any analytical progress with the path integration is difficult, when the steric term is included. Instead, to estimate the effects of undulations, we adapt a simpler approach used in Refs. [14,21,32]. The steric confinement of a WLC molecule can be estimated quite well by constructing a harmonic pseudopotential that tries to reproduce steric confinement [32]. Following Refs. [14,21], we estimate both maximum and minimum cutoffs for fluctuations in $R(s)$ within the braid, $d_{\rm min}$ and $d_{\rm max}$. There, indeed, should be a maximum displacement for braid undulations. This is because pulling the braid apart at one location causes tightening of the braid at another location due to the elastic response and the braid geometry (see Fig. 2).

To see how we introduce these cutoffs, let us first start by defining $r(s) = R(s) - R_0$, where $\langle R(s)\rangle = R_0$ is the mean braid diameter. For $r(s) > d_{\rm max}$ we replace $r(s)$ in both the elastic and electrostatic energies with $d_{\rm max}$, and for $r(s) < d_{\rm min}$ we replace $r(s)$ with $d_{\rm min}$, but we leave all derivatives of $r(s)$ untouched. This procedure prevents an unphysical overestimation (or underestimation) of the average bending and electrostatic energies when we replace the steric interaction term with the harmonic potential [32]. The true steric interaction potential never allows for values of elastic bending energy and electrostatic energy without these cutoffs, where $r(s) < d_{\rm min}$ or $r(s) > d_{\rm max}$.

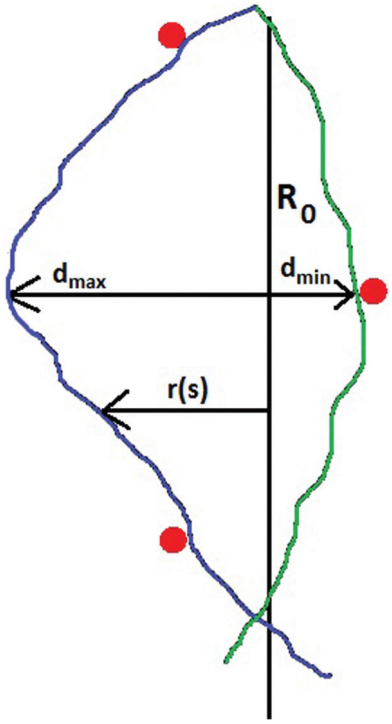

FIG. 2. (Color online) Schematic picture of confinement of a molecule by the other molecule in the braid. Here the red (gray) dots represent the confining molecule. The vertical spacing between dots is the superhelical pitch P. The blue (dark gray) line represents a trajectory of the molecule that results in $d_{\rm max}$, the maximum distance in $r(s)$. The green (gray) line represents a trajectory that results in $d_{\rm min}$, the minimum distance in $r(s)$. The straight vertical black line represents the mean position of the molecule at $R(s) = R_0$.

Following the above procedure, we can write down an approximate form for the total energy functional

$$\begin{aligned} E_T[R(s),\eta(s),\Delta\Phi(s)] \approx\ & \tilde{E}_{\rm elst}[R(s),\eta(s),\Delta\Phi(s)] \\ & + \tilde{E}_{\rm int}[R(s),\eta(s),\Delta\Phi(s)] \\ & + \tilde{E}_{\rm st}[r(s)], \end{aligned} \tag{2.33}$$

where for the steric contribution we now have the harmonic pseudopotential

$$\begin{aligned} \tilde{E}_{\rm st}[r(s)] &= k_BT \int_{-\infty}^{\infty} ds \frac{k_0}{2}[R(s) - R_0]^2 \\ &= k_BT \int_{-\infty}^{\infty} ds \frac{k_0}{2} r(s)^2. \end{aligned} \tag{2.34}$$

For the elastic energy contribution we write

$$\tilde{E}_{\rm elst}[R(s),\eta(s),\Delta\Phi(s)] \approx k_BT\int_{-L/2}^{L/2} ds\{\mathsf{E}_{\rm elst}[\Delta\Phi'(s),R''(s),R'(s),R_0+d_{\rm min},\eta'(s),\eta(s)]\theta[d_{\rm min}-r(s)] + \mathsf{E}_{\rm elst}[\Delta\Phi'(s),R''(s),R'(s),R_0+r(s),\eta'(s),\eta(s)]\theta[d_{\rm max}-r(s)]\theta[r(s)-d_{\rm min}] + \mathsf{E}_{\rm elst}[\Delta\Phi'(s),R''(s),R'(s),R_0+d_{\rm max},\eta'(s),\eta(s)]\theta[r(s)-d_{\rm max}]\}. \quad (2.35)$$

For the interaction energy we may write

$$\tilde{E}_{\rm int}[R(s),\eta(s),\Delta\Phi(s)] \approx k_BT\int_{-L/2}^{L/2} ds\{\mathsf{E}_{\rm int}[\Delta\Phi(s),R_0+d_{\rm min},\eta(s)][\theta(d_{\rm min}-r(s)] + \mathsf{E}_{\rm int}[\Delta\Phi(s),R_0+r(s),\eta(s)] \times\theta[r(s)-d_{\rm min}]\theta[d_{\rm max}-r(s)] + \mathsf{E}_{\rm int}[\Delta\Phi(s),R_0+d_{\rm max},\eta(s)]\theta[r(s)-d_{\rm max}]\}. \quad (2.36)$$

For $d_{\rm min}$ we may simply choose $2a-R_0$, estimating $d_{\rm max}$ is a little trickier for a braid. In the braid, one can consider one of the molecules as wrapping around the other to form a cage (Fig. 2) and vice versa. The simplest assumption is to assume that this cage can be approximated by a hard walled cylinder, and so set $r_{\rm max}\approx R-2a$ [3]. We think, however, that this may overestimate the degree of maximum mutual confinement of the molecules within a tight braid, i.e., when $P\gg R-2a$, where P is the pitch of the braid. To estimate what $d_{\rm max}$ might be, we consider the unlikely case of trajectories that are unaffected by electrostatics, for one of the molecules. Such trajectories, described by $R(s)$, deviate away from R_0 in a wormlike chain fashion. The maximum accumulation in $R(s)$ is limited by the steric repulsion at another point along the braid (Fig. 2), as the molecule must always return back inside the cage of the other molecule. This suggests that the molecule should be deflected back over a length $\lambda_{\rm max}$ that is of the order of P, i.e.,

$$\lambda_{\rm max}\sim P=\pi R_0/\tan(\eta_0/2), \quad (2.37)$$

where $\eta_0=\langle\eta(s)\rangle$. If the steric confinement can be estimated through a harmonic pseudopotential, this suggests that we may obtain an a crude estimate for $d_{\rm max}$ by using the classic scaling formula [19] for a wormlike chain confined in a harmonic potential

$$\lambda_B=\left(\sqrt{2}d^2l_p^b\right)^{1/3}, \quad (2.38)$$

which relates the standard deflection length λ_B of a molecule to the root mean fluctuation amplitude d (see Refs. [14,19]). Here, the root mean fluctuation amplitude d is for trajectories untouched by the interaction potential and therefore seems a reasonable choice for an estimate of $d_{\rm max}$, as only these trajectories are likely to reach a maximum value of $r(s)$. Thus, combining both Eq. (2.37) and Eq. (2.38) replacing λ_B with $\lambda_{\rm max}$, we obtain the estimate

$$d_{\rm max}\approx\left(\frac{\pi R_0}{\tan(\eta_0/2)}\right)^{3/2}\frac{1}{\left(l_p^b\sqrt{2}\right)^{1/2}}. \quad (2.39)$$

We find that, for all the cases examined in the Results section, in all of Eqs. (2.33)–(2.36) we can effectively set $d_{\rm max}$ to infinity. This is because the estimated value of $d_{\rm max}$ from Eq. (2.39) is sufficiently large for its difference from $d_{\rm max}=\infty$ to be tiny in the average bending and electrostatic energies, which are used in the calculation. Regardless of how we estimate $d_{\rm max}$, the criterion for setting $d_{\rm max}=\infty$ is that $d_{\rm max}\gg d_r=\langle r(s)^2\rangle^{1/2}$. If the electrostatic confinement is sufficiently strong, this criterion will be satisfied.

Another important difference from Ref. [14] is in how we estimate the effective spring constant of the harmonic term [Eq. (2.34)]. We suppose that the mean squared displacement, when considering only steric interactions, is determined by an average of $d_{\rm max}$ and $-d_{\rm min}$. Therefore, in terms of path integration over $r(s)$, we may write

$$\langle r(s)^2\rangle_{\rm str}=\frac{\int Dr(s)r(s)^2\exp\left[-\frac{E_{\rm str}[r(s)]}{k_BT}\right]}{\int Dr(s)\exp\left[-\frac{E_{\rm str}[r(s)]}{k_BT}\right]} \approx (d_{\rm max}-d_{\rm min})^2/2, \quad (2.40)$$

where we use the energy functional

$$E_{\rm str}[r(s)]=\frac{k_BT}{2}\int_{-\infty}^{\infty}ds\left[\frac{l_p^b}{2}\left(\frac{d^2r(s)}{ds^2}\right)^2+k_0r(s)^2\right] \quad (2.41)$$

in the Boltzmann weight of Eq. (2.40). From Eqs. (2.40) and (2.41), we estimate the effective spring constant to be

$$k_0\approx\frac{2}{(d_{\rm max}-d_{\rm min})^{8/3}\left(l_p^b\right)^{1/3}}. \quad (2.42)$$

F. Variational calculation of the free energy

Following Ref. [14], we then construct a variational principle. Here, we build the following effective energy functional $d_{\rm max}$,

$$E_{\rm eff}[r(s),\delta\eta(s),\delta\Phi(s)] = k_BT\left(\int_{-\infty}^{\infty}ds\left[\frac{l_p^b}{4}\left(\frac{d^2r(s)}{ds^2}\right)^2+\frac{k_rr(s)^2}{2}\right] + \int_{-\infty}^{\infty}ds\left[\frac{l_p^b}{4}\left(\frac{d\delta\,\eta(s)}{ds}\right)^2+\frac{k_\alpha\delta\eta(s)^2}{2}\right] + \int_{-\infty}^{\infty}ds\left[\frac{l_p^h}{4}\left(\frac{d\delta\,\Phi(s)}{ds}\right)^2+\frac{k_\Phi\delta\Phi(s)^2}{2}\right]\right), \quad (2.43)$$

where $\Delta\Phi(s)=\Delta\Phi_0(s)+\delta\Phi(s)$ and $\eta(s)=\eta_0+\delta\eta(s)$. Here, $\delta\Phi(s)$, $\delta\eta(s)$, and $r(s)$ are the thermal fluctuations about

the mean fields $\Delta\Phi_0(s)$, η_0, and R_0, respectively. We write down a variational form for $\Delta\Phi_0(s)$, where both η_0 and R_0 are assumed constant with respect to s (as in Ref. [1]), which is

$$\Delta\Phi_0(s) = \Delta\bar{\Phi} + \frac{\sigma_H}{2\langle h\rangle}\int_{-L/2}^{L/2}\frac{\Delta\Omega(s')(s-s')}{|s-s'|} \times \exp\left(-\frac{|s-s'|}{\lambda_h}\right), \tag{2.44}$$

where λ_h is the helical adaptation length. To understand what this length means, we consider the correlation function $C(s-s') = \langle[\Delta\Phi(s) - \Delta\Phi(s')]^2\rangle$. This correlation function describes the accumulation of the mismatch between the two molecular helices in the braid. For $s - s' \ll \lambda_h$ $C(s-s')$ grows linearly with increasing $|s-s'|$, but when $s - s' \gg \lambda_h$, $C(s-s')$ stops growing and stays constant [14]. The adaptation length decreases with the increasing strength of the helix-dependent forces.

We then calculate the variational free energy [14]

$$F_T = -k_BT\ \ln\ Z_{\rm eff} + \langle\langle E_T[R(s),\eta(s),\Delta\Phi(s)] - E_{\rm eff}[r(s),\delta\eta(s),\delta\Phi(s)]\rangle_0\rangle_{\Delta\Omega}, \tag{2.45}$$

where

$$Z_{\rm eff} = \int D\delta\Delta\Phi(s)\int D\delta\eta(s)\int Dr(s)\exp\left(-\frac{E_{\rm eff}[r(s),\delta\eta(s),\delta\Phi(s)]}{k_BT}\right) \tag{2.46}$$

and the thermal average is given by

$$\langle E_T - E_{\rm eff}\rangle_0 = \frac{1}{Z_{\rm eff}}\int D\delta\Phi(s)\int D\delta\eta(s)\int Dr(s)\,(E_T - E_{\rm eff})\exp\left(-\frac{E_{\rm eff}[r(s),\delta\eta(s),\delta\Phi(s)]}{k_BT}\right). \tag{2.47}$$

Appearing in both Eqs. (2.46) and (2.47) are functional integrals that describe the product of integrations taken at each point s with respect to $\delta\Phi$, $\delta\eta$, and r, thereby summing over all the available degrees of freedom. The averaging can be performed (see Appendix B of [24]) yielding the following energy function [where Eqs. (2.26)–(2.30) have been used]:

$$\begin{aligned}\frac{F_T}{Lk_BT} = {}& \frac{F_c}{Lk_BT} + \frac{l_p^b}{R_0^2}f(R_0,d_r;a)\left[\frac{3}{2} - 2\cos\eta_0\exp\left(-\frac{\lambda_\eta}{2l_p^b}\right) + \frac{\cos2\eta_0}{2}\exp\left(-\frac{2\lambda_\eta}{l_p^b}\right)\right] \\ & + \frac{2l_B(1-\theta)^2}{l_c^2}\frac{g_0[\kappa_DR_0,\kappa_Dd_r,(R_0-2a)/d_r]}{[\kappa_Da K_1(\kappa_Da)]^2} - \frac{4l_B}{l_c^2}\frac{[\zeta_1(f_1,f_2,\theta)]^2}{[\kappa_1aK_1'(\kappa_1a)]^2}\cos\Delta\bar{\Phi}\ \exp\left(-\frac{\lambda_h^*}{2\lambda_c}\right) \\ & \times\left\{g_0[\kappa_1R_0,\kappa_1d_r,(R_0-2a)/d_r] + (\bar{g}/\kappa_1)\sin\eta_0\exp\left(-\frac{\lambda_\eta}{2l_p^b}\right)g_1[\kappa_1R_0,\kappa_1d_r,(R_0-2a)/d_r]\right\} \\ & + \frac{4l_B}{l_c^2}\frac{[\zeta_2(f_1,f_2,\theta)]^2}{[\kappa_2aK_2'(\kappa_2a)]^2}\cos2\Delta\bar{\Phi}\ \exp\left(-\frac{2\lambda_h^*}{\lambda_c}\right) \\ & \times\left\{g_0[\kappa_2R_0,\kappa_2d_r,(R_0-2a)/d_r] + (4\bar{g}/\kappa_2)\sin\eta_0\exp\left(-\frac{\lambda_\eta}{2l_p^b}\right)g_1[\kappa_2R_0,\kappa_2d_r,(R_0-2a)/d_r]\right\} \\ & + \frac{2l_B}{l_c^2}\sum_{n=-\infty}^{\infty}\frac{g_{\rm img}[n,\kappa_nR_0,\kappa_nd_r,(R_0-2a)/d_r;a]}{[\kappa_naK_n'(\kappa_na)]^2}[\zeta_n(f_1,f_2,\theta)]^2\end{aligned} \tag{2.48}$$

and

$$\frac{F_c}{Lk_BT} = \frac{3}{2^{8/3}d_r^{2/3}\left(l_p^b\right)^{1/3}} + \frac{1}{4\lambda_\eta} + \frac{\left(l_p^h+\lambda_c\right)^2}{16\lambda_h^*\lambda_cl_p^h} + \frac{d_r^2}{(d_{\rm max}-d_{\rm min})^{8/3}\left(l_p^b\right)^{1/3}}, \tag{2.49}$$

where

$$f(R_0,d_r;a) \simeq \frac{R_0}{d_r\sqrt{2\pi}}\int_{[(2a/R_0)-1]}^{\infty}dx\,\frac{1}{(1+x)^2}\exp\left[-\frac{x^2}{2}\left(\frac{R_0}{d_r}\right)^2\right] + \frac{1}{2}\frac{R_0^2}{(2a)^2}\left[1-\mathrm{erf}\left(\frac{1}{\sqrt{2}}\frac{R_0-2a}{d_r}\right)\right], \tag{2.50}$$

$$\begin{aligned}g_j\,[\kappa_nR_0,\kappa_Dd_r,(R_0-2a)/d_r] = {}& \frac{1}{\sqrt{2\pi}}\int_{(2a-R_0)/d_r}^{\infty}dy\,K_j(\kappa_nR_0+y\kappa_nd_r)\exp\left(-\frac{y^2}{2}\right) \\ & + \frac{K_j(2\kappa_na)}{2}\left[1-\mathrm{erf}\left(\frac{1}{\sqrt{2}}\frac{R_0-2a}{d_r}\right)\right],\end{aligned} \tag{2.51}$$

$$g_{\rm img}[n,\kappa_n R_0,\kappa_n d_r,(R_0-2a)/d_r;a]$$
$$=-\frac{1}{\sqrt{2\pi}}\sum_{j=-\infty}^{\infty}\int_{(2a-R_0)/d_r}^{\infty}dy\,K_{n-j}(\kappa_n R_0+y\kappa_n d_r)K_{n-j}(\kappa_n R_0+y\kappa_n d_r)\frac{I_j'(\kappa_n a)}{K_j'(\kappa_n a)}\exp\left(-\frac{y^2}{2}\right)$$
$$-\frac{1}{2}\sum_{j=-\infty}^{\infty}K_{n-j}(2\kappa_n a)K_{n-j}(2\kappa_n a)\frac{I_j'(\kappa_n a)}{K_j'(\kappa_n a)}\left[1-\mathrm{erf}\left(\frac{1}{\sqrt{2}}\frac{R_0-2a}{d_r}\right)\right]. \tag{2.52}$$

In any other helix-specific theory that has exponential decay of the helical harmonics of the interaction force with $R(s)$, the form of Eq. (2.51) may still be justified, although the values of prefactors appearing in Eq. (2.48) may not necessarily be described through the KL theory. Both $\lambda_c^{(0)}$ and l_p^h combine in a combined coherence length $1/\lambda_c=\sigma_H/\lambda_c^{(0)}+1/l_p^h$. This combined coherence length λ_c is the length scale at which the two helices, in the absence of helix-dependent interactions, start to fall out of register. This coherence length combines mismatch due to different base-pair texts (nonhomologous molecules) with mismatch caused by thermal fluctuations. Here, we have eliminated k_Φ and k_η in favor of the adaptation lengths $\lambda_h^*=1/2[l_p^h/(2k_\Phi)]^{1/2}(1+\lambda_c/l_p^h)=\lambda_h/2(1+\lambda_c/l_p^h)$, $\lambda_\eta=[l_p^b/(2k_\eta)]^{1/2}$ and k_r in terms of the mean square fluctuation amplitude $d_r=\sqrt{\langle r(s)^2\rangle}$, which is related to k_r through

$$k_r=\frac{1}{d_r^{8/3}2^{5/3}\left(l_p^b\right)^{1/3}}. \tag{2.53}$$

We find that $\langle l_p^b\sin\eta(s)R'(s)\eta'(s)/[2R(s)]\rangle_0=0$ and we have neglected $\langle[1-\cos\eta(s)]R'(s)^2/[2R(s)^2]\rangle_0$ that arises from Eq. (2.17). This is reasonable, provided that

$$\left\langle\left(\frac{dR(s)}{ds}\right)^2\right\rangle_0\ll\frac{2\left[\frac{3}{2}-2\cos\eta_0\exp\left(-\frac{\lambda_\eta}{2l_p^b}\right)+\frac{1}{2}\cos2\eta_0\exp\left(-\frac{2\lambda_\eta}{l_p^b}\right)\right]}{1-\cos\eta_0\exp\left(-\frac{\lambda_\eta}{2l_p^b}\right)}, \tag{2.54}$$

which means that the neglected term is much smaller than $\langle[1-\cos\eta(s)]^2/R(s)^2\rangle_0$, which also contributes. In Appendix B of [24] $\langle R'(s)^2\rangle_0$ is calculated to be

$$\left\langle\left(\frac{dR(s)}{ds}\right)^2\right\rangle_0=\frac{1}{2^{1/3}}\left(\frac{d_r}{l_p^b}\right)^{2/3}=\left(\frac{d_r}{\lambda_B}\right)^2, \tag{2.55}$$

where we have used Eq. (2.38) to write things in terms of λ_B.This means that Eq. (2.54) is satisfied, as well as the assumptions that $R'(s)\ll\cos\eta(s)$, which were used to derive Eqs. (2.17) and (2.25), provided that $d_r\ll l_p$. It makes physical sense that $\langle R'(s)^2\rangle_0$ should depend on the ratio of d_r to the deflection length λ_B. Here, the deflection length is a measure of the distance over which the fluctuations in $r(s)$ accumulate, until we reach $r(s)\sim d_r$ where the molecule is deflected back, on average. As we shall see for the parameters used, $d_r\ll l_p^b$ (with the value of $l_p^b=500$ Å for DNA), and so these conditions are easily satisfied.

In Appendix C of Ref. [24], we show the equations on d_r, λ_h^*, λ_η, R_0,$\Delta\Phi$, and η_0 that arise from minimization of this free energy with respect to these variational parameters.

III. RESULTS

Here, we investigate the effects of undulations on the results of Ref. [1] for DNA. However, there is one additional difference; instead of the small angle formula for both the chiral torque and bending energy, we use trigonometric functions. We find that this only makes a slight difference to the results without undulations. The advantages of using such functions are that it makes thermal averaging easier and may provide a more rapidly convergent series in powers of $\sin\eta(s)$ when higher order corrections are considered. Nevertheless, for the purpose of comparison with Ref. [1], we choose $f_1=0.4$ and $f_2=0.6$ and Debye length $\kappa_D^{-1}=7$ Å.

A. Free energy

In Fig. 3(a) we plot the total braiding free energy for homologous and nonhomologous DNA molecules with and without undulations as a function of the charge compensation parameter θ. This free energy is Eq. (2.48) minimized with respect to d_r, λ_η, λ_h^*, R_0, η_0, and $\Delta\bar{\Phi}$. For the braid to be stable $F<0$; otherwise the braid corresponds to a metastable state and the unpaired state of two isolated molecules (which has $F=0$) predominates. We see that the main effect of undulations is to raise the threshold value of θ at which the paired and the unpaired states have the same energy; we call this value θ_c. For homologous molecules, including undulations increases θ_c from $\approx$0.6 to $\approx$0.7, and for nonhomologous molecules from $\theta_c\approx0.7$ to $\approx$0.8. The main cause of this shift in θ_c is the contribution to the free energy F_c due to the reduction in entropy, when the molecules are electrostatically confined within the braided conformation. To see this we have plotted in Fig. 3(b) this contribution for the various cases considered in Fig. 3(a). Without undulations [1], in Eq. (2.48) we set $d=0$,

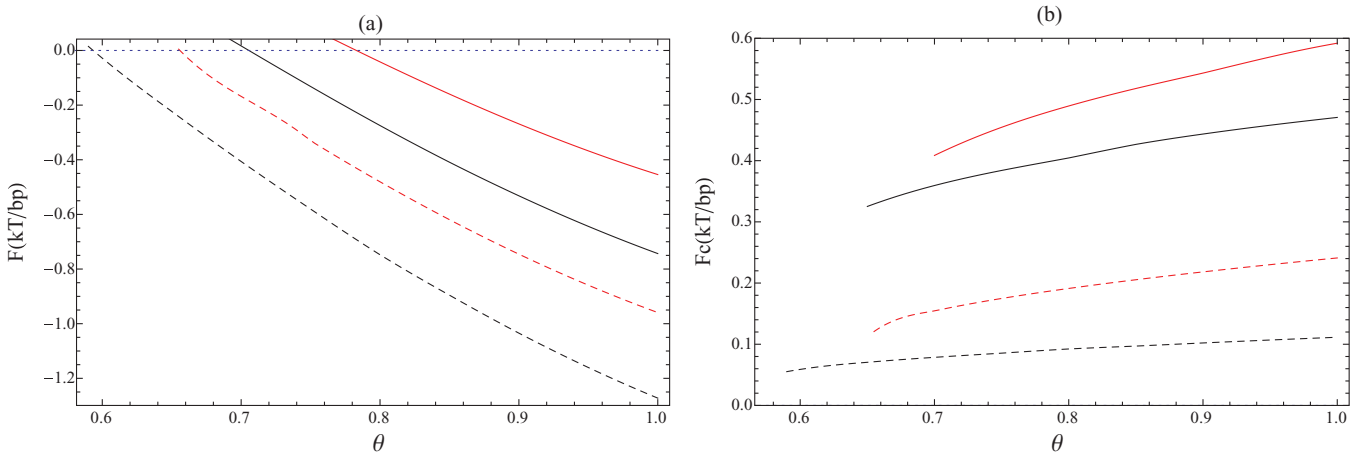

FIG. 3. (Color online) Braid confinement entropy increases the threshold attraction for spontaneous braid formation. We plot (a) the total pairing free energy and (b) the confinement free energy [see Eqs. (2.49) and (3.1)]. Both are plotted as functions of the overall charge compensation θ with $f_1 = 0.4$, $f_2 = 0.6$, and $\kappa_D^{-1} = 7$ Å. The black curves are for a pair of homologous molecules and the red (gray) curves are for nonhomologous molecules. The dashed lines are for the case without undulations (as in Ref. [1]) and the solid lines are with undulations. We see that the confinement entropy is much larger when undulations are considered, increasing the value of θ above which the braid becomes stable.

$\lambda_\eta = 0$ and F_c is given by

$$\frac{F_c}{Lk_BT} = \frac{(l_p^h + \lambda_c)^2}{16\lambda_h\lambda_c l_p^h}. \tag{3.1}$$

In both Eqs. (2.49) and (3.1) we use the optimized values for λ_h,d, and λ_η (see Fig. 4).

B. Fluctuation parameters

Looking at Fig. 4, we see the following trends. As we increase θ, the parameters λ_h,d, and λ_η all decrease, meaning that the fluctuations in $\Delta\Phi(s)$, $R(s)$, and $\eta(s)$ all diminish. These trends drive an increasing entropy loss, due to confinement, with increasing θ. This results in the increase in the confinement free energy seen in Fig. 3(b) as θ grows. Also, both d and λ_η are quite small, which accounts for this contribution to the total free energy being large [Fig. 3(b)]. The size of d_r is due to the strong electrostatic interactions, while the smallness of λ_η arises from the quite large bending rigidity terms that depend on $\eta(s)$. In Fig. 4(a), we see that undulations have little effect on the value of λ_h^*; they only slightly increase λ_h^* and this increase diminishes as θ gets larger. This trend is completely consistent with both d_r and λ_η both decreasing with increasing θ, as λ_h^* without undulations is determined with both $d = 0$ and $\lambda_\eta = 0$. In all cases, nonhomologous molecules have the largest values of λ_h^*/λ_c, d, and λ_η at fixed θ; this is because they have the largest degree of fluctuations due to intrinsic structural helix disorder, suppressing helix-specific electrostatic interactions.

C. Mean structural parameters

Now, let us examine the mean structural parameters. We find that $\bar{\Phi} \approx \pi/2$; it only increases very slightly as θ increases, and changes very little with undulations. Last of all, in Fig. 5, we show R_0,η_0, and P, which are the mean braid diameter, tilt angle, and supercoil pitch, respectively. As θ increases, R_0 decreases, whereas η_0 increases, thereby causing a decrease in the supercoiling pitch of the braid. The reason why η_0 increases is simple; as we increase the value of θ while keeping $f_1 = 0.4$ and $f_2 = 0.6$ fixed, we make the variation in the surface charge density as we move along the molecular surface, from positive to negative values, more pronounced. This means that there is a stronger impetus for the two molecules to be tilted with respect to each other, creating a stronger chiral torque [the size of the electrostatic terms in Eq. (2.25) multiplying $\sin\eta(s)$ increases]. This increased torque pushes the equilibrium value of η_0 to larger values. The reduction in R_0 can again be explained by the increase in electrostatic zipper attraction [6,33] with increasing θ, which counteracts the image charge repulsion, bending, and steric forces and pushes the two molecules closer together.

In Fig. 5, we see that the effect of undulations is to slightly raise both R_0 and P, as well as to slightly lower η_0. The balance of forces is not changed much by undulations, which is reflected by the rather low values of d and λ_η. The slight increase in R_0 can be explained by the fact that undulations cause the repulsive image charge terms in the electrostatic energy to be enhanced more than attractive terms arising from the direct electrostatic interaction. This increases the amount of repulsion from the case where there are no undulations. The values of η_0 are smaller, first because fluctuations in η weaken the chiral torque through λ_η, and secondly due to the equilibrium value of R_0 being pushed out to slightly larger values. Last of all, we observe that for homologous molecules, as opposed to nonhomologous molecules, R_0 and P are smaller and η_0 is larger. The value of R_0 is smaller for homologous molecules as the attractive helix-specific forces are stronger. This is due to the degree of large scale helical disorder λ_h^*/λ_c being smaller than that for nonhomologous molecules [see Fig. 4(a)]. The larger values of η_0 for homologous molecules is attributable, again, to the smaller value of λ_h^*/λ_c, which increases the strength of the chiral torque.

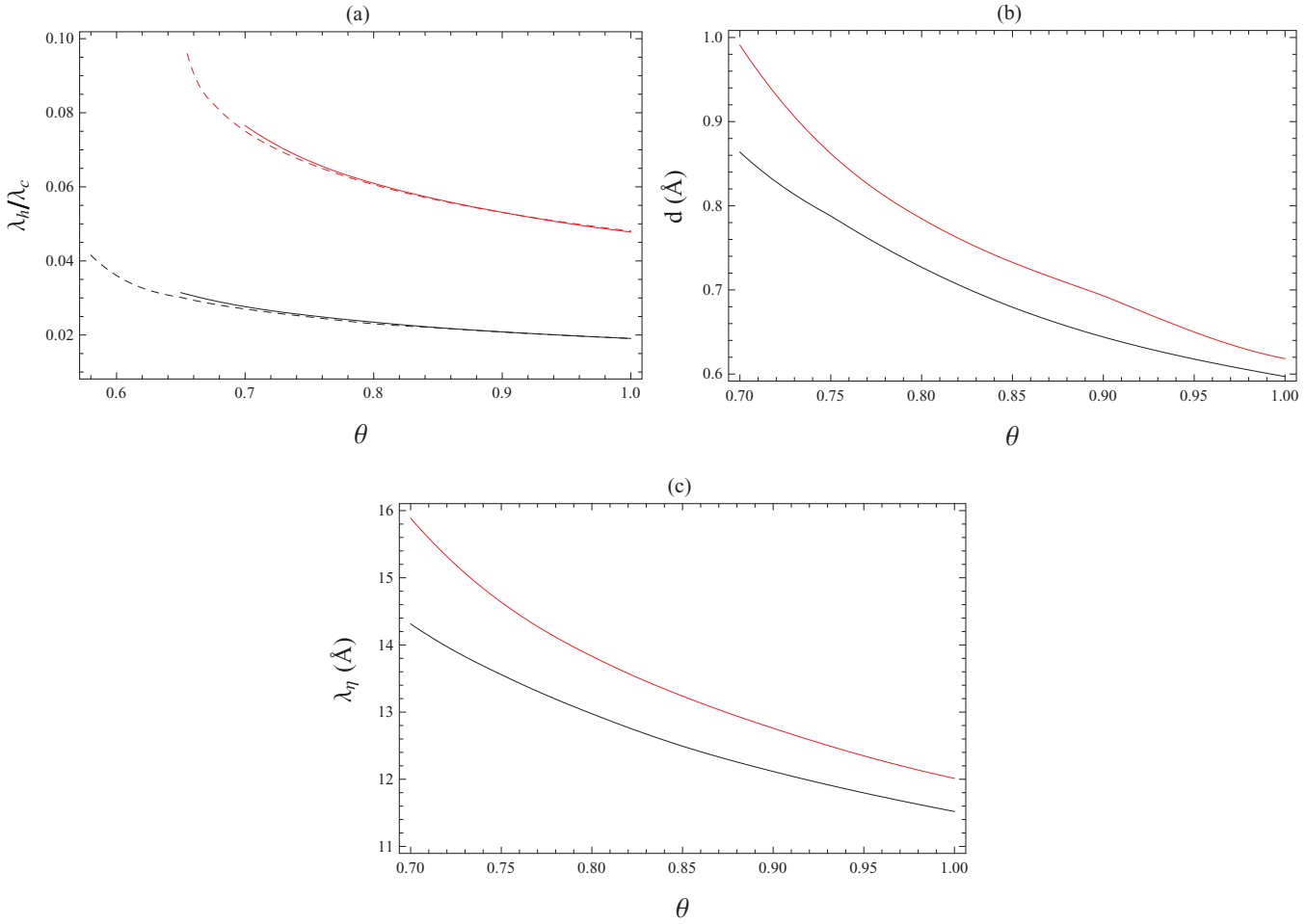

FIG. 4. (Color online) The braid fluctuation parameters. We show plots of (a) λ_h^*, the helical adaptation length, (b) d, and (c) λ_η. Again, the values $f_1 = 0.4$, $f_2 = 0.6$, and $\kappa_D^{-1} = 7$ Å are used. Again, the black curves are for a pair of homologous molecules, while the red (gray) curves are for nonhomologous molecules. The dashed lines are for the case without undulations (as in Ref. [1]) and the solid lines are with undulations. Nonhomologous molecules fluctuate more than homologous ones. d and λ_η are small due to the electrostatic confinement and the bending elasticity, respectively.

IV. DISCUSSION

In this paper, we have developed a theory to describe undulations in a braid where there are helix-dependent forces. This theory may be applied to charged helical macromolecules when their helical structure affects the interaction forces between them. We compared the results of the theory with those obtained in [1], for DNA-like charge distributions, using results calculated from the electrostatic KL theory. It was found that the effect of the undulations was to increase considerably the amount of attraction needed for a braided configuration to have lower free energy than two separated molecules. This is due to the loss of entropy from confinement. We found that when the condensed ions were all localized in the grooves the threshold value of $\theta = \theta_c$, above which the braiding state is stable, increased by 0.1, for braids formed by both nonhomologous and homologous molecules. As $\theta_c \approx 0.7$ for homologous molecules, our results suggest that, in bulk solution, braiding might only occur when divalent, if not trivalent, ions are present. We would suggest that a suitable place to search for such braided states is in ionic conditions, where DNA remains uncondensed, close to those required for DNA condensation and aggregation. There may be a narrow window in ionic conditions where spontaneous braiding may indeed occur. A braiding state may still be formed in the pairing experiments of [34]. This state might be stabilized in sodium chloride solution due to the molecular crowding effects of a large number of molecules attached to the substrate used in these experiments. Another reason might be a reduction in configurational entropy due to their attachment, so that the entropy cost for confinement of the DNA to a braid is lower. Though, there could perhaps be subtler effects due to the nature of the capillary surface, some contaminating protein [35], or divalent ions.

For plectonemes, a simple model was presented to describe chiral effects in DNA closed loops [9]. In light of the results presented here, the model presented in Ref. [9] will have to be refined to take account of undulations, as they have a significant effect. Helix nonideality was also not included in the model. In such a system a tightly wound plectoneme state competes with a loosely wound state. In the latter state chiral effects are likely not to be important, as the molecules are too far apart. Including the confinement

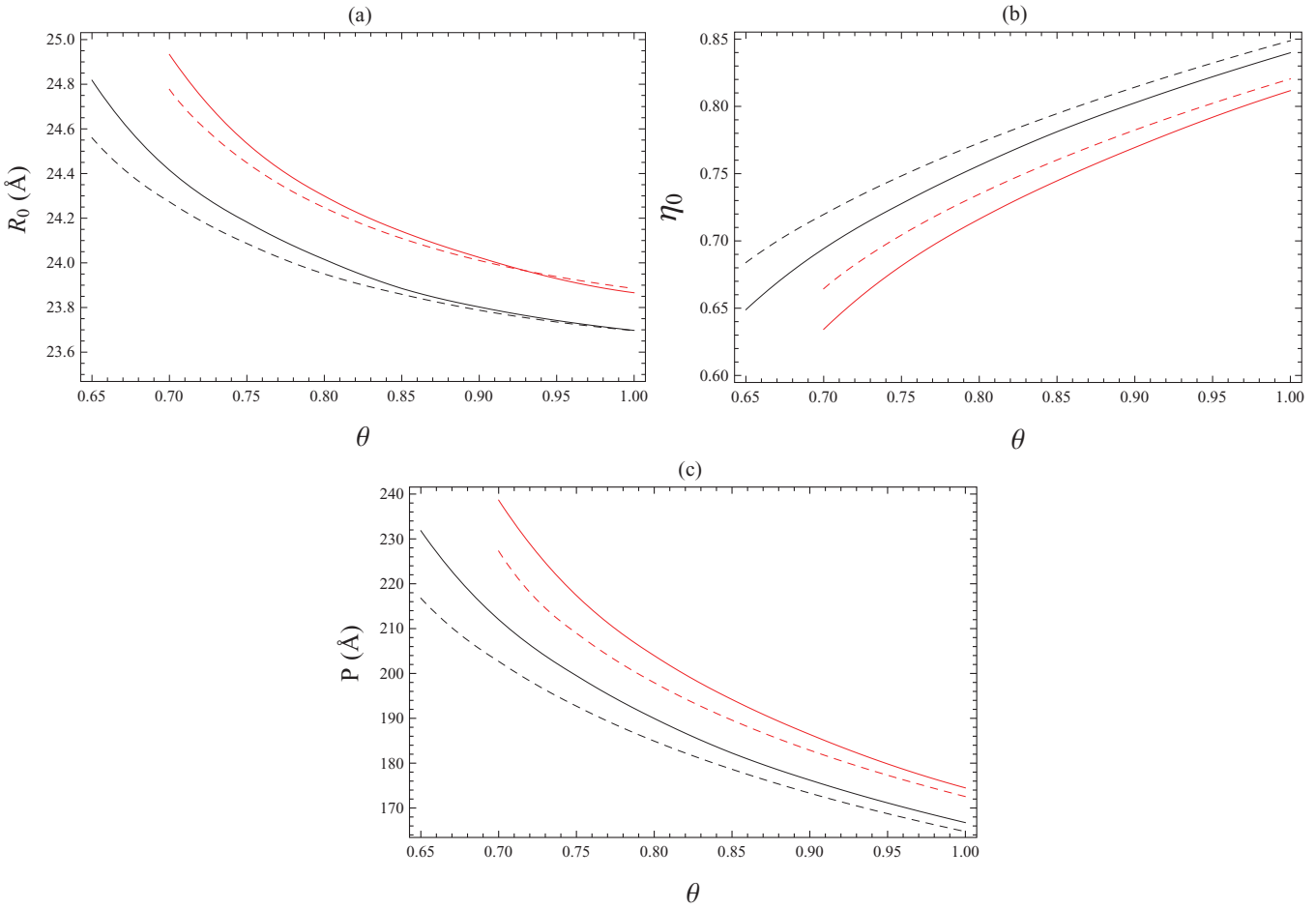

FIG. 5. (Color online) Braid structural parameters. We show plots of (a) R_0, the braid diameter, (b) η_0, the tilt angle, and (c) P, the braid supercoil pitch. Here we use the same values of the parameters and use of colors, solid and dashed lines as in the previous two figures. Undulations change both R_0 and η_0 only very slightly. The balance of forces is not significantly affected.

entropy and undulations likely favors this loosely wound state. This suggests that the asymmetry in the energy between left and right handed supercoils has been overestimated without including undulations and helix nonideality. Also, recent work [36] to do with single molecule twisting experiments [37], using the undulation theory of Ref. [3], suggests that the chiral torque, if it is present for DNA, is too strong. Part of this problem might be due to underestimating the confinement entropy. Based on the approach presented here, an undulation theory where the confinement is calculated self-consistently could be developed. However, perhaps the best experimental test, to what degree helix-specific forces are present in braids, is experiments along the lines of Ref. [10], but under different ionic conditions. Here, again, undulations of the molecules need to be estimated properly. To address these issues, we hope in a future work to modify the theory presented in this paper to closed-loop supercoils and braids under mechanical forces [9,10]. However, one should point out that to describe right handed DNA plectonemes properly, one may also have to take into account the B to Z transition, especially for GC sequences [38,39].

Currently, the calculations do not include fluctuations of the braid center line. For braids formed from uniformly charged rodlike molecules, stabilized by mechanical forces and topological constraints, such fluctuations decouple and need not be considered. However, for helix-dependent forces the braid asymmetry caused by such fluctuations couples these fluctuations to $\Delta\Phi(s)$, the relative azimuthal orientation between helices at a point s along the braid. What effect this has on the theory is yet to be seen. Indeed, we will want to include undulations of the braid axis to complete the theory. It is also possible for mechanically braided molecules, such as those considered in [10], for the braid center lines of plectonemes to buckle under large elastic stresses. In such buckling, the braid center lines may wrap around each other to form a plectonemelike structure. At present, however, the theory presented so far only deals with the average trajectory of the center line of the braid being straight.

Most of the approximations used in this paper rely on the condition $\langle R'(s)^2\rangle_0 \ll 1$. As was discussed at the end of the Theory section, this condition relies on the mean square undulation amplitude d_r being much less than the bending persistence length l_p^b. This should be noted when trying to extend this approach to other interaction theories, physical situations, or different molecules. We also used a smooth cylinder approximation that we think is valid for the strong confining forces that we consider, though we should point out that the equilibrium separation of the braid $R_0 \approx 24$ Å is rather

close. Indeed, one might expect that the steric contribution of the phosphate ridges might play a role. However, the electrostatic interactions (as considered in the KL theory) try to align the two molecules so that phosphate ridges sit inside the grooves of the other molecule, as does the steric interaction. Probably, electrostatic interactions predominate over steric ones, as the two molecules are highly confined by such electrostatic forces. But, perhaps, if helix-specific forces are weaker than what the KL calculations predict, or behave differently (like the correlation forces discussed below), the steric effects of the phosphate ridges may be more important. A simple way of modeling this effect might be to make the effective spring constant k_0, appearing in the harmonic pseudopotential for the steric interaction, dependent on the averages $\langle\cos\Delta\Phi(s)\rangle$, $\langle\cos 2\Delta\Phi(s)\rangle$, and $\langle\sin\eta(s)\rangle$. This would take account of the fact that $a_{\rm steric}$, the minimum separation between center lines, would change with the relative orientation of the molecules, whereas for smooth cylinders considered here $a_{\rm steric} = a$. One then would also have a minimum value of a and values of $\Delta\Phi$ and η where this value is realized. We suggest that this would be equivalent [at order $\sin\eta(s)$] to writing an effective steric interaction of the form given by Eq. (2.25), but with the coefficients having power law dependence, as opposed to an exponential dependence through modified Bessel functions.

Of course, equilibrium separations $R_0 \approx 24$ Å are too close for the theory of [5], based on a bulk dielectric response, to be quantitatively valid. One of the hopes behind this study was that undulations would push up the value of R_0 considerably, but this effect seems to be quite small; the confinement entropy matters much more. Therefore, instead of Eqs. (2.26)–(2.30), perhaps a better approach would be to obtain empirical forms for $E_{\rm img}(R)$, $E_0^{(n)}(R)$, and $E_1^{(n)}(R)$ from simulation data with realistic groove binding potentials and counterion structure [40]. Another way of improving the theory might be to introduce terms of order $\sin^2\eta(s)$ into Eq. (2.25). These terms are likely to be repulsive in nature and should limit the value of η_0, as well as push R_0 outwards. The origin of such terms is that there is a tilt angle favored by helix-specific interactions alone through the geometry of the DNA. These interactions do not favor an unlimitedly large tilt angle. Nevertheless, the approach presented in this paper could easily be modified to reflect such refinements in the interaction energy, if helical structure does indeed matter.

It may also be theoretically interesting and insightful to redo these calculations for interaction potentials in the strong coupling limit [7], where correlations between ions are strong. In such theories, instead of an electrostatic zipper, one has a correlation zipper [8]. Though the effects of helical adaptation will be more or less described by the same theory as described here [the form of the interaction energy should be the same as what is given in Eq. (2.25)], the azimuthal alignment will be of the opposite sense to that of the electrostatic zipper [6,33]; the phosphates of both molecules want to come close to each other, instead of trying to be as far apart as possible, so as to generate the strongest correlation forces. It would be intriguing to see what effect this has on the formation and structure of the braid.

ACKNOWLEDGMENTS

D.J.L. would like to acknowledge useful discussions with A. A. Korynshev and R. Cortini and thanks A. M. Sartor for reading the manuscript. He would also like to acknowledge the support of the Human Frontiers Science Program (Grant No. RGP0049/2010-C102). This work has also been inspired by joint work that has been supported by the United Kingdom Engineering and Physical Sciences Research Council (Grant No. EP/H004319/1).

[1] R. Cortini, A. A. Kornyshev, D. J. Lee, and S. Leikin, Biophys. J. **101**, 875 (2011).
[2] Y. Timsit and P. Varnai, PLoS ONE **5**, e9326 (2010); Nucl. Acids Res. **38**, 4163 (2010).
[3] J. F. Marko and E. D. Siggia, Phys. Rev. E **52**, 2912 (1995).
[4] J. Ubbink and T. Odijk, Biophys. J. **76**, 2502 (1999).
[5] A. A. Kornyshev and S. Leikin, J. Chem. Phys. **107**, 3656 (1997).
[6] A. A. Kornyshev, D. J. Lee, S. Leikin, and A. Wynveen, Rev. Mod. Phys. **79**, 943 (2007), and references contained therein.
[7] M. Kanduč, J. Dobnikar, and R. Podgornik, Soft Matter **5**, 868 (2009).
[8] D. J. Lee, J. Phys.: Condens. Matter **23**, 105102 (2011).
[9] R. Cortini, D. J. Lee, and A. A. Kornyshev, J. Phys.: Condens. Matter **24**, 162203 (2012).
[10] G. Charvin, A. Vologodskii, D. Bensimon, and V. Croquette, Biophys. J. **88**, 4124 (2005).
[11] D. C. Rau and V. A. Parsegian, Biophys. J. **61**, 246 (1992).
[12] D. C. Rau and V. A. Parsegian, Biophys. J. **61**, 260 (1992).
[13] B. A. Todd, V. A. Parsegian, A. Shirahata, T. J. Thomas, and D. C. Rau, Biophys. J. **94**, 4775 (2008).
[14] D. J. Lee, A. Wynveen, A. A. Kornyshev, and S. Leikin, J. Phys. Chem. B **114**, 11668 (2010).
[15] A. A. Kornyshev, D. J. Lee, S. Leikin, A. Wynveen, and S. B. Zimmerman, Phys. Rev. Lett. **95**, 148102 (2005).
[16] A. Leforestier and F. Livolant, Proc. Natl. Acad. Sci. U.S.A. **106**, 9157 (2009).
[17] F. Gentile, M. Moretti, T. Limongi, A. Falqui, G. Bertoni, A. Scarpellini, S. Santoriello, L. Maragliano, R. P. Zaccaria, and E. di Fabrizio, Nano Lett. **12**, 6453 (2012).
[18] R. Podgornik, D. C. Rau, and V. A. Parsegian, Biophys. J. **66**, 962 (1994).
[19] T. Odijk, Biophys. Chem. **46**, 69 (1993).
[20] J. V. Selinger and R. F. Bruinsma, Phys. Rev. A **43**, 2922 (1991).
[21] D. J. Lee, S. Leikin, and A. Wynveen, J. Phys.: Condens. Matter **22**, 072202 (2010).
[22] E. Starostin and G. Van der Heijden (unpublished) http://www.ucl.ac.uk/ ∼ucesgvd/braids.html.
[23] D. J. Lee, arXiv:1302.1420.
[24] See Supplemental Material at http://link.aps.org/supplemental/10.1103/PhysRevE.88.022719 for derivation of the energy functional, formulas for energy averaging, and minimization of free energy.

[25] J. Lipfert, J. W. J. Kerssemakers, T. Jager, and N. H. Dekker, Nat. Methods **7**, 977 (2010).
[26] V. A. Bloomfied, D. M. Crothers, and I. Tinoco, Jr., *Nucleic Acids, Structures, Properties, and Functions* (University Science Books, Sausalito, CA, 2000).
[27] We should also point out that the elasticity constants for DNA are sequence dependent so that we have the functions $B(s)$, $C_t(s)$, and $C_s(s)$. However, we expect that over length scales larger than a few base pairs, these functions can be replaced by their average values.
[28] A. Wynveen, D. J. Lee, A. Kornyshev, and S. Leikin, Nucl. Acids Res. **36**, 5540 (2008).
[29] A. Wynveen, D. J. Lee, A. Kornyshev, and S. Leikin, Nucl. Acids Res. **39**, 7289 (2011).
[30] W. J. Duffin, *Electricity and Magnetism* (McGraw-Hill, New York, 1990).
[31] C. A. Davey and T. J. Richmond, Proc. Natl. Acad. Sci. U.S.A. **99**, 11169 (2002).
[32] W. Helfrich and W. Harbich, Chem. Scr. **25**, 32 (1985).
[33] A. A. Kornyshev and S. Leikin, Phys. Rev. Lett. **82**, 4138 (1999).
[34] C. Danilowicz, C. H. Lee, K. Kim, K. Hatch, V. W. Coljee, N. Kleckner, and M. Prentiss, Proc. Natl. Acad. Sci. U.S.A. **106**, 19824 (2009).
[35] N. Shurr (private communication).
[36] R. Cortini (unpublished).
[37] Q. Shao, S. Goyal, L. Finzi, and D. Dunlap, Macromolecules, **45**, 3188 (2012).
[38] F. Azorin, A. Nordheim, and A. Rich, EMBO J. **2**, 649 (1983), and references contained therein.
[39] C. Singleton, J. Klysik, S. Stirdivant, and R. Wells, Nature (London) **299**, 312 (1982).
[40] It is difficult to ascertain whether the basic form of Eq. (2.25), but with different coefficients, can be applied in the case of bridging interactions due to coordination complexes formed by some multivalent ions. However, we would speculate that the strength of these interactions is probably likely to depend on the azimuthal alignment of the phosphate ridges. This would suggest Eq. (2.25), based on symmetry considerations, might still be useful. But, such a justification lies beyond the scope of this paper.